Nanotechnology, Science and Applications

Dovepress
open access to scientific and medical research

Open Access Full Text Article

ORIGINAL RESEARCH

Synthesis, characterization, and in vitro evaluation of novel polymer-coated magnetic nanoparticles for controlled delivery of doxorubicin

This article was published in the following Dove Press journal:
Nanotechnology, Science and Applications
3 February 2012
Number of times this article has been viewed

Abolfazl Akbarzadeh[1]
Nosratollah Zarghami[2]
Haleh Mikaeili[3]
Davoud Asgari[4]
Amir Mohammad Goganian[5]
Hanie Khaksar Khiabani[5]
Mohammad Samiei[6]
Soodabeh Davaran[3]

[1]Department of Medicinal Chemistry, Tabriz University of Medical Sciences, [2]Department of Clinical Biochemistry and Laboratory Medicine, Division of Medical Biotechnology, Faculty of Medicine, Tabriz University of Medical Sciences, [3]Tuberculosis and Lung Disease Research Center, Tabriz University of Medical Sciences, [4]Research Center for Pharmaceutical Nanotechnology, Tabriz University of Medical Sciences, [5]Department of Organic Chemistry, Faculty of Chemistry, University of Tabriz, [6]Faculty of Dentistry, Tabriz University of Medical Sciences, Tabriz, Iran

Abstract: Poly (N-isopropylacrylamide-methacrylic acid, PNIPAAm-MAA)-grafted magnetic nanoparticles were synthesized using silane-coated magnetic nanoparticles as a template for radical polymerization of N-isopropylacrylamide and methacrylic acid. Properties of these nanoparticles, such as size, drug loading efficiency, and drug release kinetics, were evaluated in vitro for targeted and controlled drug delivery. The resulting nanoparticles had a diameter of 100 nm and a doxorubicin-loading efficiency of 75%, significantly higher doxorubicin release at 40°C compared with 37°C, and pH 5.8 compared with pH 7.4, demonstrating their temperature and pH sensitivity, respectively. In addition, the particles were characterized by X-ray powder diffraction, scanning electron microscopy, Fourier transform infrared spectroscopy, and vibrating sample magnetometry. In vitro cytotoxicity testing showed that the PNIPAAm-MAA-coated magnetic nanoparticles had no cytotoxicity and were biocompatible, indicating their potential for biomedical application.

Keywords: magnetic nanoparticles, drug loading, doxorubicin release, biocompatibility

Introduction

Magnetic nanoparticles are a major class of nanoscale materials with the potential to revolutionize current clinical diagnostic and therapeutic techniques.[1] Due to their unique physical properties and ability to function at the cellular and molecular level of biological interactions, magnetic nanoparticles are being actively investigated as the next generation of magnetic resonance imaging contrast agents[2] and as carriers for targeted drug delivery.[3,4] Although early research in the field can be dated back several decades, the recent surge of interest in nanotechnology has significantly expanded the breadth and depth of research into magnetic nanoparticles. With a wide range of applications in the detection, diagnosis, and treatment of illnesses, such as cancer,[5] cardiovascular disease,[6] and neurological disease,[7–10] magnetic nanoparticles may soon play a significant role in meeting the health care needs of tomorrow (Figure 1).

As therapeutic tools, magnetic nanoparticles have been evaluated extensively for targeted delivery of pharmaceuticals through magnetic drug targeting,[11–16] and by active targeting through attachment of high affinity ligands.[17–19] With the ability to utilize magnetic attraction and/or specific targeting of disease biomarkers, magnetic nanoparticles offer an attractive means of remotely directing therapeutic agents specifically to a disease site, while simultaneously reducing dosage and the deleterious side effects associated with nonspecific uptake of cytotoxic drugs by healthy tissue.

Also referred to as magnetic targeted carriers, colloidal iron oxide particles in early clinical trials have demonstrated some degree of success with the technique

Correspondence: Soodabeh Davaran
Tuberculosis and Lung Disease Research Center, Tabriz University of Medical Sciences, Tabriz, Iran
Tel +98 41 133 7225
Fax +98 41 1334 4798
Email davaran@tbzmed.ac.ir

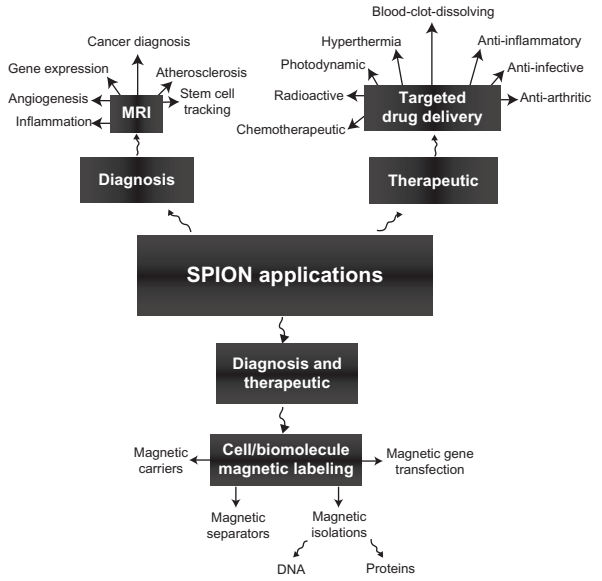

Figure 1 Applications of superparamagnetic iron oxide nanoparticles.
Abbreviation: SPION, superparamagnetic iron oxide nanoparticle.

and shown satisfactory tolerability in patients.[20–22] Although not yet capable of reaching levels of safety and efficacy for regulatory approval, preclinical studies indicate that some of the shortcomings of magnetic drug targeting technology, such as poor penetration depth and diffusion of the released drug from the disease site, can be overcome by improvements in magnetic targeted carrier design.[23,24]

Furthermore, the use of magnetic nanoparticles as carriers in multifunctional nanoplatforms as a means of monitoring of drug delivery is an area of interest.[25,26] A significant challenge associated with the application of these magnetic nanoparticle systems is their behavior in vivo. The efficacy of many of these systems is often compromised due to recognition and clearance by the reticuloendothelial system prior to reaching the target tissue, as well as by an inability to overcome biological barriers, such as the vascular endothelium or the blood–brain barrier. The fate of these magnetic nanoparticles upon intravenous administration is highly dependent on their size, morphology, charge, and surface chemistry.

The physicochemical properties of nanoparticles directly affect their subsequent pharmacokinetics and biodistribution.[27] To increase the effectiveness of magnetic nanoparticles, several techniques, including reducing size and grafting nonfouling polymers, have been used to improve their "stealthiness" and increase their blood circulation time to maximize the likelihood of reaching targeted tissues.[28,29] The major disadvantage of most chemotherapeutic approaches to cancer treatment is that most are nonspecific. Therapeutic (generally cytotoxic) drugs are administered intravenously, leading to general systemic distribution.[30–33]

The nonspecific nature of this technique results in the well known side effects of chemotherapy because the cytotoxic drug attacks normal healthy cells in addition to its primary target, ie, tumor cells.[34–41] To overcome this great disadvantage, magnetic nanoparticles can be used to treat tumors in three different ways: specific antibodies can be conjugated to the magnetic nanoparticles to bind selectively to related receptors and inhibit tumor growth; targeted magnetic nanoparticles can be used for hyperthermia tumor therapy; and drugs can be loaded into magnetic nanoparticles for targeted therapy.[42–45] Targeted delivery of antitumor agents adsorbed on the surface of magnetic nanoparticles is a promising alternative to conventional chemotherapy (Figure 2).

Particles loaded with the drug are concentrated at the target site with the aid of an external magnet. The drugs are then released in the desired area. Magnetic particles smaller than 4 μm are eliminated by cells of the reticuloendothelial system, mainly in the liver (60%–90%) and spleen (3%–10%). Particles larger than 200 nm are usually filtered to the spleen, the cutoff point of which extends up to 250 nm, while particles up to 100 nm are mainly phagocytosed by liver cells.

In general, the larger the particles are, the shorter their plasma half-life.[47] Functionalization of magnetic nanoparticles with amino groups, silica, polymers, various surfactants, or other organic compounds is usually performed in order to achieve better physical and chemical properties. Moreover, the core/shell structure of magnetic nanoparticles has the advantages of good dispersion, high stability against oxidation, and an appreciable amount of drug can be loaded into the polymer shell. Furthermore, lots of functional groups from polymers on the surface can be used

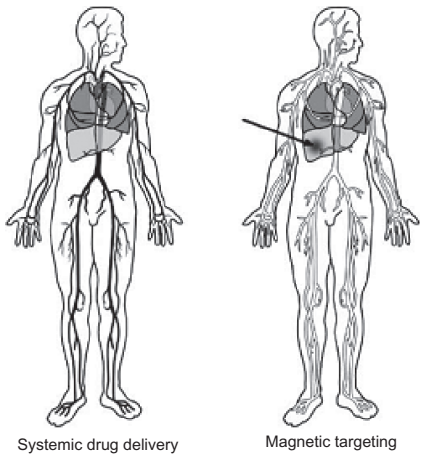

Figure 2 Concept of magnetic drug targeting.

for further functionalization to obtain various properties.[48] It is preferable that magnetic nanoparticles retain sufficient hydrophilicity and, with coating, do not exceed 100 nm in size to avoid rapid clearance by the reticuloendothelial system.[49] It has been found that surface functionalization also plays a key role in nanoparticle toxicity.

In this research we investigated the in vitro characteristics of our nanoparticles for drug delivery application.[50] Of these temperature-sensitive polymer-coated magnetic nanoparticles, poly-N-isopropylacrylamide (PNIPAAm)-coated magnetic nanoparticles are of particular interest because of their stimuli (temperature) responsiveness and enhanced drug-loading ability. These characteristics are due to their large inner volume, amphiphilicity, capacity for manipulation of permeability, and response to an external temperature stimulus with an on–off mechanism. However, one potential problem with using PNIPAAm as a polymer coat is that its lower critical solution temperature, ie, the temperature at which a phase transition occurs, is below body temperature (32°C). To increase the lower critical solution temperature of PNIPAAm above body temperature, it has been copolymerized with different monomers.[51,52]

Two synthetic steps were used to manufacture magnetic nanoparticles coated with PNIPAAm and methacrylic acid (MAA).[53] First, magnetic nanoparticles were covalently bound with vinyltriethoxysilane, a silane coupling agent, to produce a template site for radical polymerization. NIPAAm and MAA were then polymerized on the silicon layer around the magnetic nanoparticles via methylene-bis-acrylamide and ammonium persulfate as a cross-linking agent and an initiator, respectively. The resultant particles were characterized by X-ray powder diffraction, scanning electron microscopy, Fourier transform infrared spectroscopy, and vibrating sample magnetometry. The in vitro cytotoxicity test for the PNIPAAm-MAA-coated magnetic nanoparticles was analyzed. The drug release behavior of doxorubicin (an anticancer drug model) in the nanoparticles at various pH levels and at temperatures below and at the lower critical solution temperature was also analyzed. Being able to monitor the location of drug-loaded nanoparticles after administration would be a considerable advantage in situations such as cancer therapy, in which drugs have serious side effects in healthy tissue.[1,54]

Materials and methods

Materials

Ferric chloride hexahydrate ($FeCl_3 \cdot 6H_2O$), ferrous chloride tetrahydrate ($FeCl_2 \cdot 4H_2O$), ammonium hydroxide (25 wt%, and other chemicals of analytical grade were purchased from Fluka (Buchs, Switzerland). 1,4 dioxan, ammonium persulfate, AIBN (2 azobisisobutyronitrile), MAA, NIPAAm, methylene-bis-acrylamide (BIS), vinyltriethoxysilane, acetic acid, and ethanol were purchased from Sigma-Aldrich (St Louis, MO) and used as received. Doxorubicin hydrochloride was purchased from Sigma-Aldrich. X-ray powder diffraction using a Rigaku D/MAX-2400 X-ray diffractometer with Ni-filtered Cu Kα radiation and scanning electron microscopy measurements were conducted using a VEGA/TESCAN. Drug-loading capacity and release behavior were determined using an ultraviolet 2550 spectrophotometer (Shimadzu, Japan, Tokyo). The infrared spectra of copolymers were recorded on a Perkin Elmer 983 infrared spectrophotometer (Perkin Elmer, Boston, MA) at room temperature. Magnetic properties were measured on a VSM/AGFM (Meghnatis Daghigh Kavir Co, Iran) vibrating sample magnetometer at room temperature.

Synthesis of superparamagnetic magnetite nanoparticles

Superparamagnetic magnetite (Fe_3O_4) nanoparticles were prepared using an improved chemical coprecipitation method. According to this method, 3.1736 g of $FeCl_2 \cdot 4H_2O$ (0.016 mol) and 7.568 g of $FeCl_3 \cdot 6H_2O$ (0.028 mol) were dissolved in 320 mL of deionized water, such that $Fe^{2+}/Fe^{3+} = 1/1.75$. The mixed solution was stirred under N_2 at 80°C for one hour. Then, 40 mL of $NH_3 \cdot H_2O$ was injected into the mixture rapidly, stirred under N_2 for another hour, and cooled to room temperature. The precipitated particles were washed five times with hot water and separated by magnetic decantation (Figure 3). Finally, the magnetic nanoparticles were dried under vacuum at 70°C.[55]

Preparation of vinyltriethoxysilane-coated magnetic nanoparticles

The magnetic nanoparticles were coated with vinyltriethoxysilane via acid catalyst hydrolysis, followed by electrophilic substitution of ferrous oxide on the surface as shown in our previous study. In brief, 0.49 mL of vinyltriethoxysilane was hydrolyzed

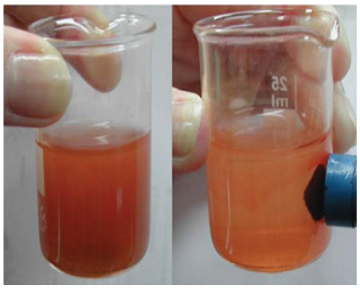

Figure 3 Magnetite-hexane suspension attached to a magnet.

using 3 mL of acetic acid in the presence of water and ethanol (1:100 vol/vol). A measured quantity (0.075 g) of magnetic nanoparticles was then dispersed by sonication at 100 W for 30 minutes in this solution. After 18 hours of vigorous mechanical stirring at room temperature (22°C–25°C), vinyltriethoxysilane-coated magnetic nanoparticles were obtained, washed with a mixture of water and ethanol (1:100 vol/vol) and collected using an external magnet. The particles were dispersed in water before the next step.

Immobilization of PNIPAAm-MAA on magnetic nanoparticles

Vinyltriethoxysilane-coated magnetic nanoparticles were used as a template to polymerize PNIPAAm-MAA in 1,4 dioxan. BIS was used as a cross-linking agent. In brief, 0.03 g of vinyltriethoxysilane-coated magnetic nanoparticles, 0.15 g of NIPAAm, 0.013 g of MAA, and 0.0135 g of BIS were sonicated in 100 mL of cold water for 45 minutes. Then, 0.08 g of ammonium persulfate was added to the solution, and the reaction was carried out at room temperature under N_2 gas for 5 hours. The product was purified several times with deionized water by using a magnet to collect only the PNIPAAm-MAA-coated magnetic nanoparticles. PNIPAAm-coated magnetic nanoparticles were also formulated using the same synthesis process as for PNIPAAm-MAA-coated magnetic nanoparticles, but without addition of MAA monomer (Figure 4).[57]

Synthesis of hybrid nanoparticles

Doxorubicin was used as a model drug in our drug-loading and drug-release experiments. In brief, 5 mg of freeze-dried PNIPAAm-MAA-coated magnetic nanoparticles and 2.5 mg of doxorubicin were dispersed in 30 mL of phosphate buffer solution. The solution was stirred at 5°C for 3 days.

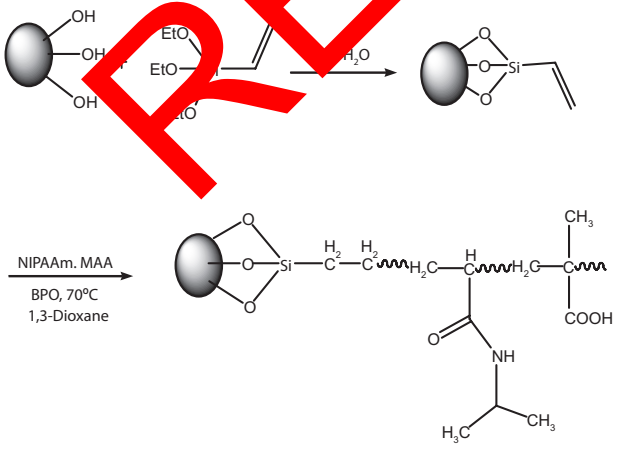

Figure 4 Chemical modification of Fe_3O_4 surface by grafting polymerization.
Abbreviations: NIPAAm, N-isopropylacrylamide; MAA, methyl methacrylic acid.

The doxorubicin-loaded PNIPAAm-MAA-coated magnetic nanoparticles were separated from the solution using an external magnet. The solution was then analyzed using an ultraviolet-visible spectrofluorometer (Shimadzu) to determine the amount of nonencapsulated doxorubicin (λ_{ex} 470 nm and λ_{em} 585 nm). This value was then compared with the total amount of doxorubicin added to determine the doxorubicin-loading efficiency of the nanoparticles.[57]

In vitro drug-release kinetics

To study drug release, four different sets of experiments were performed. These included two temperatures (40°C and 37°C) and two pH levels (5.8 and 7.4). In each drug-release experiment, 3.0 mg of the drug carrier bonded with smart polymer was sealed in 50 mL of Na_2HPO_4–NaH_2PO_4 buffer solution at a pH of 5.8 or 7.4. The test tube with a closer was placed in a water bath maintained at 40°C up to the lower critical solution temperature (37°C (higher than the lower critical solution temperature). The release medium (about 3 mL) was withdrawn at predetermined time intervals (1, 2, 3, 4, 5, 6, 7, 8, 9, 12, 24, 36, 48, 60, 80, 100, 130, 160, 190, and 220 hours). Thereafter, the samples were analyzed using an ultraviolet-visible spectrometer (Shimadzu) to determine the amount of doxorubicin released (λ_{ex} 470 nm and λ_{em} 585 nm for doxorubicin measurement).[58,59]

Cell culture

In vitro cytotoxicity and cell culture study

An A549 lung cancer cell line (kindly donated by the Pharmaceutical Nanotechnology Research Center, Tabriz University of Medical Sciences, Tabriz, Iran) were cultured in RPMI 1640 (Gibco, Invitrogen, Paisley, UK) supplemented with 10% heat-inactivated fetal bovine serum (Gibco), 2 mg/mL sodium bicarbonate, 0.05 mg/mL penicillin G (Serva Co, Tübingen, Germany), and 0.08 mg/mL streptomycin (Merck Co, Germany), and incubated at 37°C with humidified air containing 5% CO_2. After culturing a sufficient amount of cells, the cytotoxic effect of PNIPAAm-MAA-coated magnetic nanoparticles was studied by MTT assay at 24, 48 and 72 hours.[60] Briefly, 1000 cells/well were cultivated in a 96-well plate (Figure 5). After 24 hours of incubation at 37°C in a humidified atmosphere containing 5% CO_2, the cells were treated with serial concentrations of doxorubicin-loaded PNIPAAm-MAA-coated magnetic nanoparticles (0 mg/mL to 0.57 mg/mL) for 24, 48 and 72 hours in a quadruplicate manner. Control cells received 0 mg/mL extract + 200 µL of culture medium containing 10% dimethylsulfoxide. After incubation, the medium in all wells was exchanged with fresh

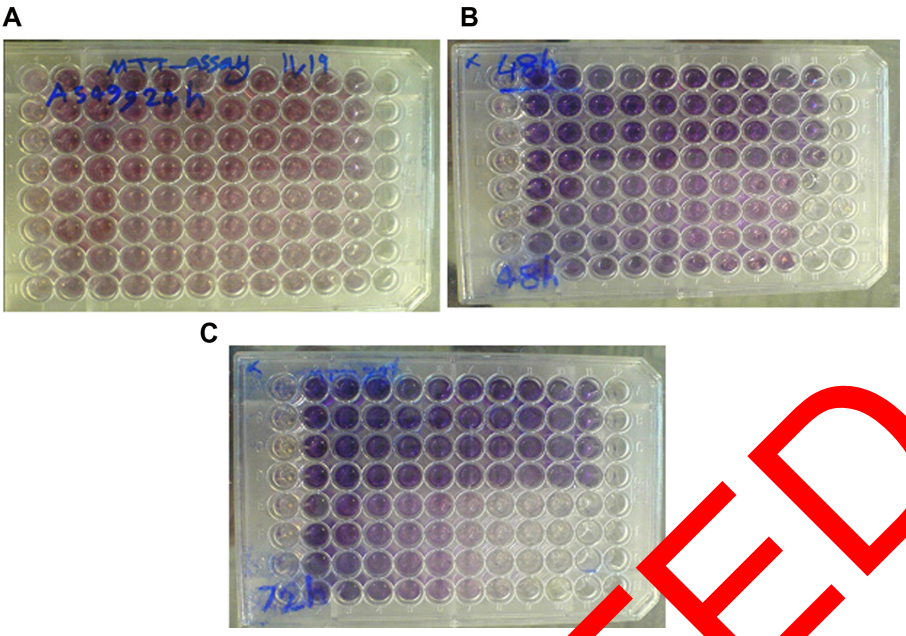

Figure 5 Cytotoxic effect of PNIPAAm-MAA-coated magnetic nanoparticles on A549 lung cancer cell line after 24 hours (**A**), 48 hours (**B**), and 72 hours (**C**) of exposure.
Abbreviations: PNIPAAm, poly (N-isopropylacrylamide); MAA, methyl methacrylic acid.

medium, and the cells were left for 24 hours in an incubator. The medium in all the wells was then removed carefully, and 50 µL of 2 mg/mL MTT dissolved in phosphate buffer solution was added to each well and the plate was covered with aluminum foil and incubated for 4.5 hours. After removing the contents of the wells, 200 µL of pure dimethylsulfoxide was added to the wells. Then, 25 µL of Sorenson's glycine buffer was added, and the absorbance of each well was immediately read at 570 nm using an EL × 800 microplate absorbance reader (Bio-Tek Instruments, Winooksi, VT) with a reference wavelength of 630 nm (Figure 5).[61]

Cell treatment

After determination of the IC_{50}, 1×10^6 cells were treated with serial concentrations of doxorubicin-loaded PNIPAAm-MAA-coated magnetic nanoparticles (0.028, 0.057, 0.114, 0.142, 0.171, and 0.199 mg/mL). For control cells, the same volume of 10% dimethylsulfoxide without the doxorubicin-loaded PNIPAAm-MAA-coated magnetic nanoparticles was added to the flask containing control cells. The culture flasks were then incubated for 24 hours at 37°C in a humidified atmosphere containing 5% CO_2 (Figure 6).

Characterization

The infrared spectra were recorded using a Fourier transform infrared spectrophotometer (FT-IR, Nicolet NEXUS 670; ThermoScientific, Waltham, MA), and the sample and KBr were pressed to form a tablet. The magnetization curves of the samples were measured using vibrating sample magnetometry (Meghnatis Daghigh Kavir Co) at room temperature. Powder X-ray diffraction (Rigaku D/MAX-2400 X-ray diffractometer with Ni-filtered Cu Kα radiation) was used to investigate the crystal structure of the magnetic nanoparticles. The infrared spectra of the copolymers were recorded on a Perkin Elmer 983 infrared spectrometer (Perkin Elmer) at room temperature. The size and shape of the nanoparticles were determined using a scanning electron microscope (VEGA/TESCAN), whereby a sample was dispersed in ethanol and a small drop was spread onto a 400 mesh copper grid.

Results

Synthesis of PNIPAAm-MAA-coated Fe_3O_4 nanoparticles

The processes for synthesis of PNIPAAm-MAA-coated Fe_3O_4 nanoparticles and the loading of doxorubicin onto them are shown in Figure 4. The Fe_3O_4 nanoparticles were prepared by chemical coprecipitation of Fe^{2+} and Fe^{3+} ions under alkaline conditions. The concentration ratio of Fe^{2+}/Fe^{3+} was selected to be 1:1.8 rather than the stoichiometric ratio of 1:2, because Fe^{2+} is prone to oxidation and becoming Fe^{3+} in solution. Fe_3O_4 nanoparticles prepared by the coprecipitation method have a number of hydroxyl groups on the surface from being in contact with the aqueous phase. Vinyltriethoxysilane-modified Fe_3O_4 nanoparticles were achieved by the reaction between vinyltriethoxysilane and the hydroxyl groups on the surface of magnetite. Two reactions were involved in the process.

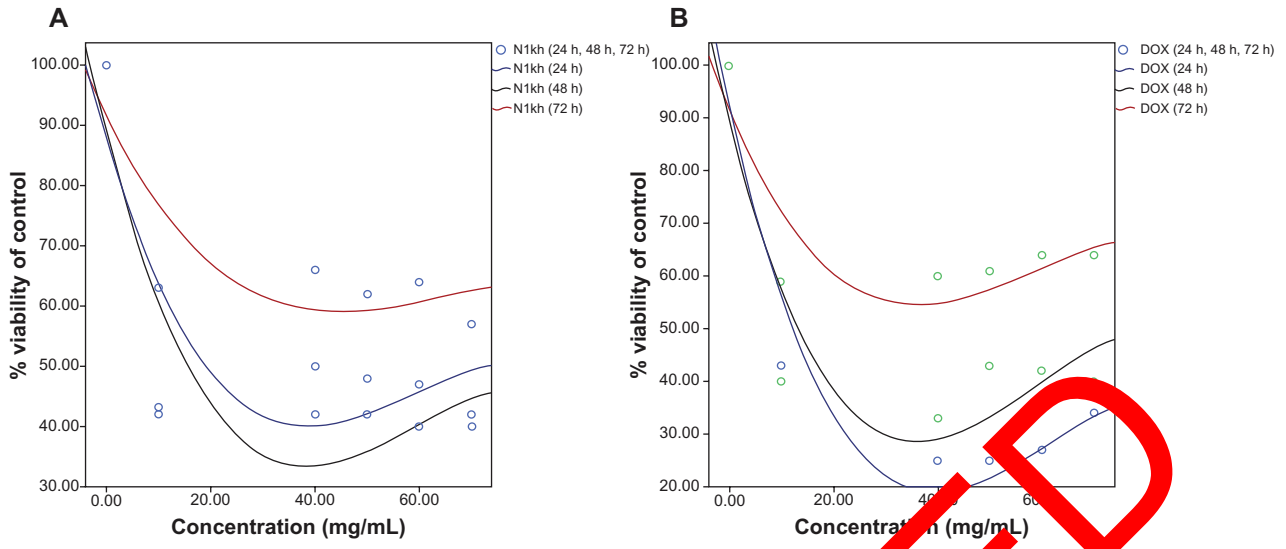

Figure 6 IC_{50} of (**A**) doxorubicin-loaded PNIPAAm-MAA-coated magnetic nanoparticles and (**B**) pure doxorubicin on A549 tumor cell line after 24, 48, and 72 hours of treatment.
Abbreviations: DOX, doxorubicin; PNIPAAm, poly (N-isopropylacrylamide); MAA, methyl methacrylic acid.

First, the vinyltriethoxysilane was hydrolyzed to highly reactive silanol species in the solution phase under alkaline conditions. Their condensation with surface free —OH groups of magnetite to form stable Fe—O—Si bonds then takes place. Oligomerization of the silanols in solution occurs as a competing reaction, with their covalent binding to the surface. Surface-grafted polymerization by NIPAAm and MAA also involves two reactions which take place simultaneously. Graft polymerization occurs on the surface of the vinyltriethoxysilane-modified Fe_3O_4 nanoparticles, while random polymerization takes place in the solution. In order to decrease random polymerization, the following strategies were adopted. After azobisisobutyronitrile was dissolved in the modified nanoparticle-suspended solution, the solution was kept overnight for the nanoparticles to absorb as much azobisisobutyronitrile as possible onto the surface. An optimal concentration of initiator was selected, BIS was used as cross-linking agent, and the monomers were added dropwise in the reaction. The unreacted oligomers were separated by magnetic decantation after the reaction.

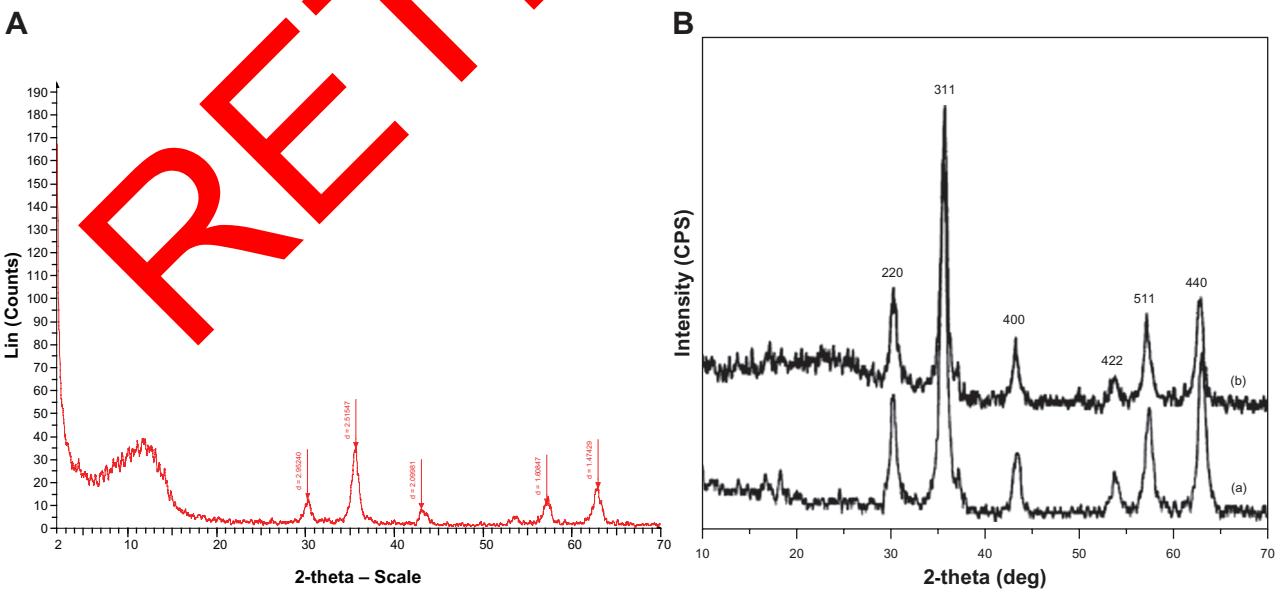

Figure 7 X-ray diffraction patterns of (**A**) pure Fe_3O_4 nanoparticles and (**B**) PNIPAAm-MMA-grafted Fe_3O_4 nanoparticles.
Abbreviations: PNIPAAm, poly (N-isopropylacrylamide); MAA, methyl methacrylic acid.

Characterization of Fe_3O_4 and PNIPAAm-MAA-coated Fe_3O_4 nanoparticles

X-ray diffraction patterns

Figure 7 shows the X-ray diffraction patterns for the pure Fe_3O_4 and PNIPAAm-MAA-grafted Fe_3O_4 nanoparticles. It is apparent that the diffraction pattern of our Fe_3O_4 nanoparticles is close to the standard pattern for crystalline magnetite (Figure 7A). The characteristic diffraction peaks, marked by their respective indices (2 2 0), (3 1 1), (4 0 0), (4 2 2), (5 1 1), and (4 4 0) could be well indexed to the inverse cubic spinel structure of Fe_3O_4 (JCPDS card 85–1436), and were also observed for PNIPAAm-MAA-grafted Fe_3O_4 nanoparticles (Figure 7B). This indicates that modified graft polymerization on the surface of the Fe_3O_4 nanoparticles did not lead to any crystal phase change. The average crystalline size D was about 15 nm, obtained from the Sherrer equation:

$$D = K\lambda/(\beta \cos \theta)$$

where K is a constant, λ is the X-ray wavelength, and β is the peak width of half-maximum.

Size, morphology, and core-shell structure of nanoparticles

Scanning electron micrographs of pure Fe_3O_4 nanoparticles are shown in Figure 8A and Fe_3O_4 nanoparticles grafted by PNIPAAm-MAA are shown in Figure 8B. In Figure 8A, the nanoparticles were strongly aggregated, which was due to the nanosize of the Fe_3O_4, and were about 20–75 nm in size, according to the results of X-ray powder diffraction. After graft polymerization, the size of the particles increased to 60–100 nm, and dispersion of the particles was greatly improved (Figure 8B), which can be explained by the electrostatic repulsion force and steric hindrance between the polymer chains on the surface of the Fe_3O_4 nanoparticles.

Fourier transform infrared spectroscopy

To evaluate the effect of graft polymerization, the homopolymers and unreacted monomers were extracted in ethanol to be

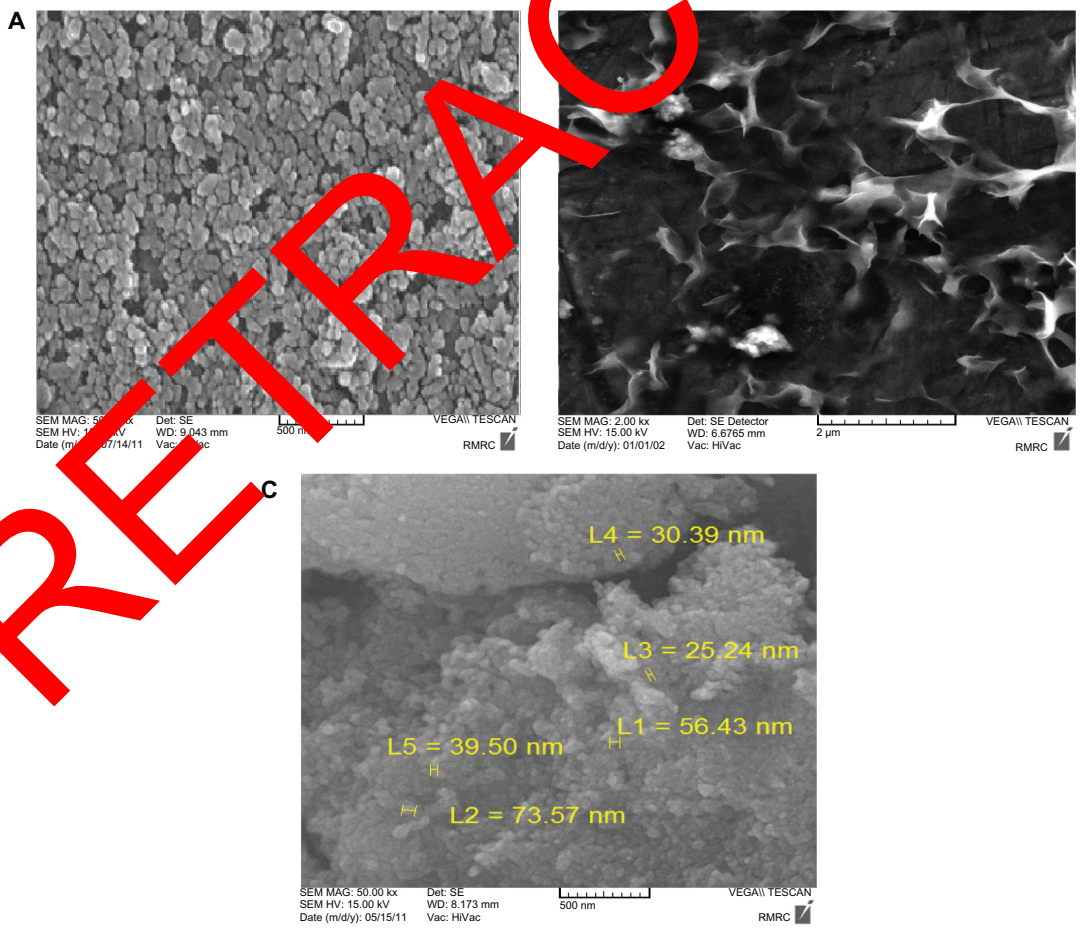

Figure 8 Scanning electron micrographs of (**A**) pure Fe_3O_4 nanoparticles (**B**) Fe_3O_4 nanoparticles grafted by PNIPAAm-MMA, and (**C**) hydrodynamic sizes of PNIPAAm-MAA-coated magnetic nanoparticles.

Abbreviations: PNIPAAm, poly (N-isopropylacrylamide); MAA, methyl methacrylic acid.

separated from the grafted nanoparticles. Fourier transform infrared spectroscopy was used to show the structure of Fe_3O_4 (Figure 9A), vinyltriethoxysilane-modified Fe_3O_4 (Figure 9B), and PNIPAAm-MAA-grafted Fe_3O_4 (Figure 9C). From the infrared spectra shown in Figure 9, the absorption peaks at 568 cm^{-1} belonged to the stretching vibration mode of Fe—O bonds in Fe_3O_4. Comparing the infrared spectra in Figure 9A and Figure 9B, vinyltriethoxysilane-modified Fe_3O_4 showed absorption peaks at 1603 and 1278 cm^{-1} attributable to the stretching vibrations of C=C and the bending vibration of Si-C bonds, a peak at 1411 cm^{-1} due to the bending vibration of the $=CH_2$ group, and additional peaks centered at 1116, 1041, 962, and 759 cm^{-1}, most probably due to the symmetric and asymmetric stretching vibration of framework and terminal Si—O— groups. All of these indicated the presence of vinyltriethoxysilane. They also indicated that the reactive groups had been introduced onto the surface of the magnetite. The absorption peaks of C=C and $=CH_2$ groups disappeared, and additional peaks at 1724, 1486, 1447 and 1387 cm^{-1} due to the stretching vibrations of C=O, the bending vibration of $—CH_2—$, —CH—, and $—CH_3$ absorption peaks at 1147, 906, and 847 cm^{-1} belonged to the stretching vibration of the alkyl groups from NIPAAm. However, identification of a peak attributable to the stretching vibrations of C—N (normally at about 1100 cm^{-1}) was problematic due to other overlapping peaks, but the element analysis method demonstrated the presence of the N element of NIPAAm in PNIPAAm-MAA-grafted Fe_3O_4 nanoparticles. Overall, these Fourier transform infrared spectra provided supportive evidence that the $–CH=CH_2$ group initiated polymerization of NIPAAm and MAA polymer chains, which were successfully grafted onto the Fe_3O_4 nanoparticle surface.

Magnetism test

The magnetic properties of the nanoparticles were analyzed using vibrating sample magnetometry at room temperature. Figure 10 shows the hysteresis loops for the samples. The saturation magnetization was found to be 34.5 and 17.6 emu/g for vinyltriethoxysilane modified Fe_3O_4 and PNIPAAm-MAA-grafted Fe_3O_4 respectively, which was less than for the pure Fe_3O_4 nanoparticles (70.9 emu/g). With its large saturation magnetization, the PNIPAAm-MAA-grafted Fe_3O_4 could be separated from the reaction medium rapidly and easily in a magnetic field. In addition, there was no hysteresis in the magnetization, with both remanence and coercivity being zero, suggesting that these magnetic nanoparticles were superparamagnetic. When the external magnetic field was removed, the magnetic nanoparticles could be well dispersed by gentle shaking. These magnetic properties are critical for applications in the biomedical and bioengineering fields.

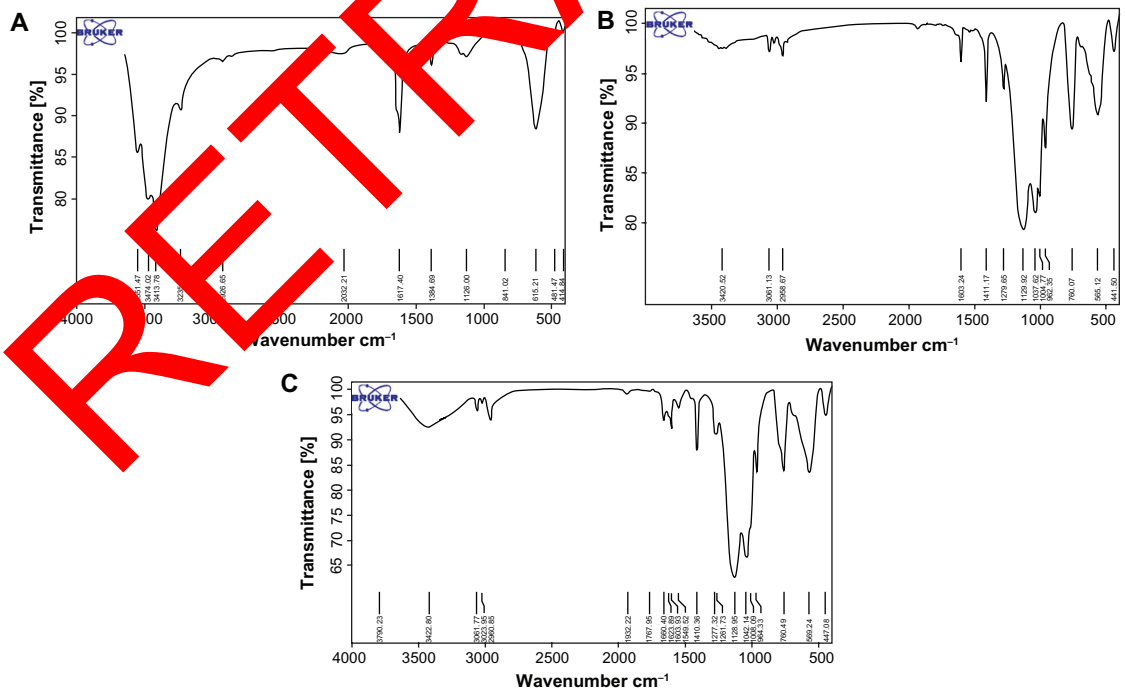

Figure 9 Fourier transform infrared spectra of (**A**) pure Fe_3O_4 nanoparticles, (**B**) Fe_3O_4 nanoparticles modified by vinyltriethoxysilane, and (**C**) PNIPAAm-MMA-grafted Fe_3O_4 nanoparticles.
Abbreviations: PNIPAAm, poly (N-isopropylacrylamide); MAA, methyl methacrylic acid.

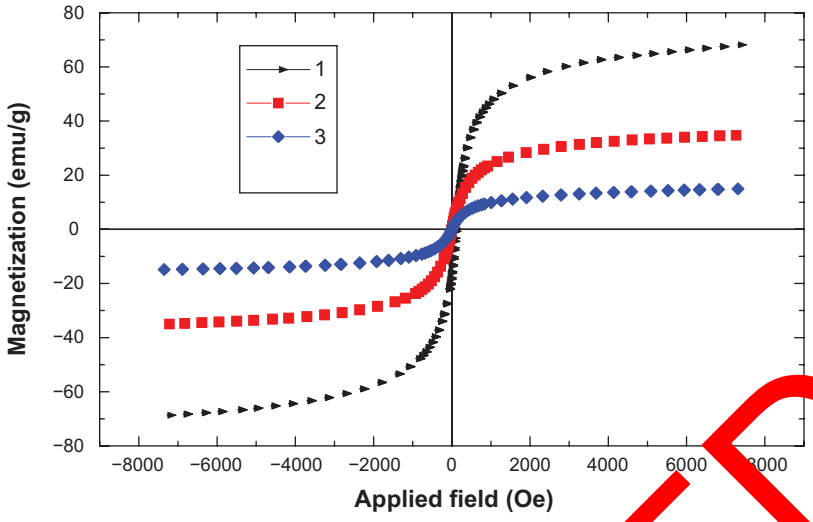

Figure 10 Magnetic behavior of magnetic nanoparticles (Fe_3O_4, VTES-Fe_3O_4, and VTES-Fe_3O_4-PNIPAAm-MAA).
Abbreviations: PNIPAAm, poly (N-isopropylacrylamide); MAA, methyl methacrylic acid; VTES, vinyltriethoxysi

Drug-loading efficiency

Doxorubicin, an anticancer drug, was used for drug-loading and drug-release studies. In brief, 20 mg of lyophilized nanoparticles and 5 mg of doxorubicin were dispersed in phosphate buffer solution. The solution was stirred at 4°C for 3 days to allow doxorubicin to entrap within the nanoparticle network. This value was then compared with the total amount of doxorubicin to determine the doxorubicin loading efficiency of the nanoparticles. The amount of nonentrapped doxorubicin in the aqueous phase was determined using an ultraviolet-visible 2550 (λ_{ex} 470 nm and λ_{em} 585 nm) spectrometer (Shimadzu). This procedure enables analysis of doxorubicin solutions with removal of most interfering substances.[62] The entrapment efficiency of doxorubicin within the nanoparticles was calculated by the difference between the total amount used to prepare the nanoparticles and the amount of doxorubicin present in the aqueous phase. Loading efficiency was calculated according to the following formula:

$$\text{Loading efficiency} = [(\text{Amount of loaded drug in mg}) / (\text{Amount of added drug in mg})] \times 100\%$$

Drug release

After 200 hours in phosphate buffer solution (0.1 M, pH 7.4, 5.8) at 37°C and 40°C, the release behavior of the nanoparticles was studied. The percentage of cumulative release of doxorubicin at 40°C was significantly higher than at 37°C (Figure 11). The pH-responsive release profiles from the hybrid nanoparticles are shown in Figure 11 (pH 5.8 and 7.4). The release rate decreased with increasing pH values. The pKa value of the amino group in doxorubicin was about 8.2. Thus, the electrostatic interaction existed in neutral surroundings and disappeared at acid surroundings. The pH of the tumor was 5.0–6.0, which is lower than the pH of normal tissue, so doxorubicin in the hybrid nanoparticles would be released at the tumor site.

In vitro cytotoxicity study

The MTT assay is an important method for evaluating the cytotoxicity of biomaterials in vitro. Using this assay, absorbance has a significant linear relationship with cell numbers. The corresponding optical images of cells are shown in Figure 12. In the current work, the MTT assay showed that doxorubicin-loaded PNIPAAm-MAA-coated magnetic nanoparticles have time-dependent but not dose-dependent cytotoxicity in an A549 lung cancer cell line

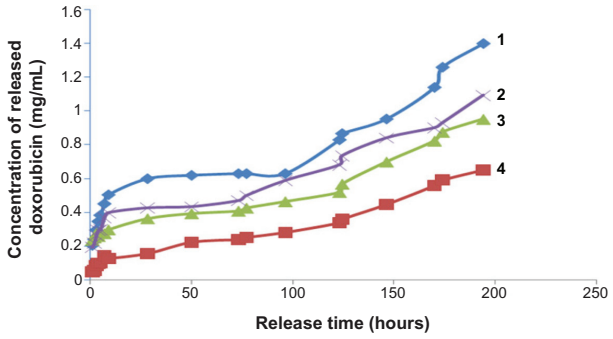

Figure 11 Release profiles of doxorubicin from the hybrid nanoparticles at different pH values. Vertical axis shows: concentration of released doxorubicin (mg/mL) and horizontal axis shows release time (hours). (**1**) pH 5.8 ± 0.01, temperature 40°C ± 0.5°C, (**2**) pH 5.8 ± 0.01, temperature 37°C ± 0.5°C, (**3**) pH 7.4 ± 0.01, temperature 40°C ± 0.5°C, (**4**) pH 7.4 ± 0.01, temperature 37°C ± 0.5°C.

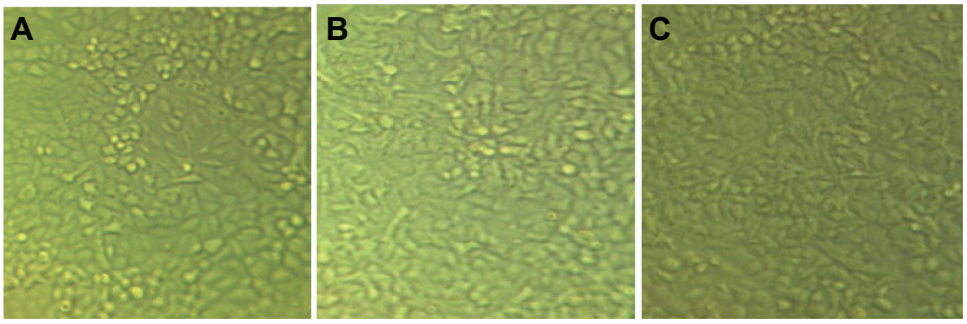

Figure 12 (**A**) Control cells, (**B**) doxorubicin-loaded PNIPAAm-MAA-coated magnetic nanoparticles, (**C**) pure doxorubicin. Morphological effect of doxorubicin-loaded PNIPAAm-MAA-coated magnetic nanoparticles in an A549 lung cancer cell line after 24 hours of treatment.
Abbreviations: PNIPAAm, poly (N-isopropylacrylamide); MAA, methyl methacrylic acid.

(IC_{50} 0.16–0.20 mg/mL). The MTT assay also showed that pure doxorubicin has dose-dependent but not time-dependent cytotoxicity in the A549 lung cancer cell line (IC_{50} 0.15 –0.16 mg/mL). Therefore, there is a need for further study of doxorubicin-loaded PNIPAAm-MAA-coated magnetic nanoparticles in an A549 lung cancer cell line in the future. However, the results of our current work demonstrate that the IC_{50} values for doxorubicin-loaded PNIPAAm-MAA-coated magnetic nanoparticles and pure doxorubicin are about 0.16, 0.20, and 0.15 mg/mL, respectively, in an A549 lung cancer cell line.

Discussion

In this work, we have characterized the in vitro behavior of PNIPAAm-MAA-coated magnetic nanoparticles for targeted and controlled drug delivery applications. The saturation magnetization was found to be 34.5 and 16 emu/g for vinyltriethoxysilane-modified Fe_3O_4 and PNIPAAm-MAA-grafted Fe_3O_4, respectively, ie, less than for the pure Fe_3O_4 nanoparticles (70.9 emu/g) by vibrating sample magnetometry. This difference suggests that a large amount of silane and polymers were coated onto the surface of the Fe_3O_4 nanoparticles. Fourier transform infrared spectroscopy was used to show the presence of Fe_3O_4, vinyltriethoxysilane-modified Fe_3O_4, and PNIPAAm-MAA-grafted Fe_3O_4. The X-ray powder diffraction data only showed peaks attributable to magnetite and revealed that modified and grafted polymerization onto the surface of Fe_3O_4 nanoparticles did not lead to crystal phase change. The size, morphology, and core-shell structure of the synthesized nanoparticles was analyzed by scanning electron microscopy. Close examination of a scanning electron microscopic image (inset in Figure 7) reveals the presence of magnetic nanoparticles (about 10 nm diameter) at the center with a PNIPAAm-MAA coating surrounding them. The size of the magnetic core was similar to earlier reported values for magnetic nanoparticles synthesized by similar methods. In comparison with PNIPAAm-coated magnetic nanoparticles, there was clearly less agglomeration of magnetic nanoparticles in the core. This might be a result of higher mixing capability due to utilization of a mechanical stirrer and the electrostatic charge repulsion from the carboxylic group of MAA in the PNIPAAm-MAA coating, which would further reduce the magnetic dipole interactions and promote stability.[63] We believe that coating magnetic nanoparticles with a biocompatible polymer is necessary when high concentrations of magnetic nanoparticles are used. The drug release study indicates that the PNIPAAm-MMA is a temperature-sensitive polymer, whereby at its lower critical solution temperature the nanoparticles go through a phase change to collapse and release more drug. After 200 hours, 60% of the bonded doxorubicin was released at 40°C, whereas at 37°C about 43% was released. The release profile for doxorubicin over the first 30 minutes is also shown in Figure 11. After 30 minutes, the percentages of cumulative release of doxorubicin were only 0.046% at 37°C, whereas at 40°C it was 2.4%. The system is shown to release its payload over a short burst release period with changes in temperature. Since the measurement time was very short while the drug release predetermined time interval was significantly large, the influence of the returned medium on drug release during the measurement time is expected to be insignificant. The doxorubicin release profiles demonstrated that our nanoparticles were sensitive to temperature, with significantly higher release at 40°C than at 37°C. The in vitro cytotoxicity test showed that the doxorubicin-loaded PNIPAAm-MAA-coated magnetic nanoparticles had no cytotoxicity and were biocompatible, which means that there is potential for biomedical application.[64] Also, the IC_{50} of doxorubicin-loaded PNIPAAm-MAA-coated magnetic nanoparticles in an A549 lung cancer cell line showed that they are time-dependent.

Conclusion

Superparamagnetic iron oxide nanoparticles were prepared via an improved chemical coprecipitation method, and magnetite (Fe_3O_4) nanoparticles were then modified by vinyltriethoxysilicane and reactive groups were introduced onto the surface of the nanoparticles. NIPAAm and MAA were then grafted onto the surface of the modified Fe_3O_4 nanoparticles by surface-initiated radical polymerization. The results indicate that the polymer chains were effectively grafted onto the surface of the Fe_3O_4 nanoparticles. The functionalized particles remained dispersive and superparamagnetic. These particles were used for encapsulation of doxorubicin under mild conditions and could be used in drug delivery. The resulting particles were characterized by X-ray powder diffraction, scanning electron microscopy, Fourier transform infrared spectroscopy, and vibrating sample magnetometry. An in vitro cytotoxicity study demonstrated that the modified Fe_3O_4 nanoparticles had no cytotoxicity and were biocompatible. This study suggests that supercritical fluid technology is a promising technique to produce drug-polymer magnetic composite nanoparticles for the design of controlled drug-release systems. Our current work demonstrates that doxorubicin-loaded, modified Fe_3O_4 nanoparticles have a potent antigrowth effect in the A549 cancer cell line and inhibits cell growth in a time dependent manner. Therefore, these nanoparticles could be natural potent chemopreventive and chemotherapeutic agents for patients with lung cancer and analogs of these nanoparticles may be appropriate candidates for drug development. Future work will include in vivo investigation of the targeting capability and effectiveness of these nanoparticles in the treatment of lung cancer.[65,66]

Acknowledgments

The authors are grateful for the financial support of the Iran National Science Foundation, Drug Applied Research Center Tabriz University of Medical Sciences, and the Department of Medicinal Chemistry at Tabriz University of Medical Sciences.

Disclosure

The authors report no conflicts of interest in this work.

References

1. Akbarzadeh A, Asgari D, Zarghami N, Mohammad R, Davaran S. Preparation and in vitro evaluation of doxorubicin-loaded Fe_3O_4 magnetic nanoparticles modified with biocompatible co-polymers. *Int J Nanomedicine*. In press.
2. Gref R, MinamitakeY, Peracchia MT, et al. Biodegradable long circulating polymeric nanospheres. *Science*. 1994;263:1600–1630.
3. Li Y, Pei Y, Zhang X, et al. PEGylated PLGA nanoparticles as protein carriers: synthesis, preparation and biodistribution in rats. *J Control Release*. 2001;71:203–211.
4. Beletsi A, Panagi Z, Avgoustakis K. Biodistribution properties of nanoparticles based on mixtures of PLGA with PLGA-PEG diblock copolymers. *Int J Pharm*. 2005;298:233–241.
5. Birnbaum DT, Brannon-Peppas L. Microparticle drug delivery systems. In: Brown DM, editor. *Drug Delivery Systems in Cancer Therapy*. New York, NY: Humana Press; 2004.
6. Eatock MM, Schätzlain A, Kaye SB. Tumor vasculature as a target for anticancer therapy. *Cancer Treat Rev*. 2000;26:191–204.
7. Avgoustakis K, Beletsi A, Panagi Z, et al. Effect of copolymer composition on the physicochemical characteristics, in vitro stability, and biodistribution of PLGA-mPEG nanoparticles. *Int J Pharm*. 2003;259:115–127.
8. Jeong Y, Nah JW, Lee HC, et al. Ad[illegible] release from flower-type polymeric micelles based on sta[illegible]lock cop[illegible]mer composed of poly (γ-benzyl L-glutamate) as the h[illegible]rophobic part a[illegible]poly(ethylene oxide) as the hydrophilic part. *Int J Pha[illegible]n*. 1999;188:4[illegible]58.
9. Jeong B, Bae YH, Kim [illegible]. Drug re[illegible]se from bi[illegible]egradable injectable thermosensitive hy[illegible]gel of PEG-P[illegible]GA-P[illegible]G triblock copolymer. *J Control Releas*[illegible]2000;63:1[illegible]163.
10. Kwon GS, Naito M, Yokoyama M, et al. Physical entrapment of adriamycin in AB block cope[illegible]er micelle[illegible]*harm Res*. 1995;12:192–195.
11. Mitra S[illegible]aur U, Ghosh[illegible] et al. Tumor targeted delivery of encapsulated ext[illegible]-doxorubicin[illegible]gate using chitosane nanoparticles as carrier. *J Co[illegible]l Release*. 2001;74:317–323.
12. Na K, Lee ES, [illegible] YH. Adriamycin loaded pullulan acetate/sulfonamide conjugate na[illegible]particles responding to tumor pH: pH-dependent cell interaction, internalization and cytotoxicity. *J Control Release*. 2003;87:[illegible]13.
13. Orive G, [illegible]rnández RM, Gasc AR, et al. Micro and nano drug delivery systems[illegible] cancer therapy. *Cancer Ther*. 2005;3:131–138.
14. [illegible]n J, Labhasetwar V. Biodegradable nanoparticles for drug and gene delivery to cells and tissue. *Adv Drug Deliv Rev*. 2003;55:329–347.
15. Banerjee SS, Chen DH. Magnetic nanoparticles grafted with cyclodextrin for hydrophobic drug delivery. *Chem Mater*. 2007;19:6345–6349.
16. Jain TK, Reddy MK, Morales MA, Leslie-Pelecky DL, Labhasetwar V. Biodistribution, clearance, and biocompatibility of iron oxide magnetic nanoparticles in rats. *Mol Pharm*. 2008;5:316–327.
17. Jain TK, Richey J, Strand M, Leslie-Pelecky DL, Flask CA, Labhasetwar V. Magnetic nanoparticles with dual functional properties: drug delivery and magnetic resonance imaging. *Biomaterials*. 2008;29:4012–4021.
18. Lai JJ, Hoffman JM, Ebara M, et al. Dual magnetic-/temperature-responsive nanoparticles for microfluidic separations and assays. *Langmuir*. 2007;23:7385–7391.
19. Hu SH, Liu TY, Liu DM, Chen SY. Nano-ferrosponges for controlled drug release. *J Control Release*. 2007;121:181–189.
20. Liu TY, Hu SH, Liu KH, Liu DM, Chen SY. Study on controlled drug permeation of magnetic-sensitive ferrogels: effect of Fe_3O_4 and PVA. *J Control Release*. 2008;126:228–236.
21. Müller-Schulte D, Schmitz-Rode T. Thermosensitive magnetic polymer particles as contactless controllable drug carriers. *J Magn Magn Mater*. 2006;302:267–271.
22. Rahimi M, Yousef M, Cheng Y, Meletis EI, Eberhart RC, Nguyen K. Formulation and characterization of a covalently coated magnetic nanogel. *J Nanosci Nanotechnol*. 2010;10(9):6072–6081.
23. Arias JL, Ruiz MA, Gallardo V, Delgado AV. Tegafur loading and release properties of magnetite/poly (alkylcyanoacrylate) (core/shell) nanoparticles. *J Control Release*. 2008;125:50–58.
24. Gupta AK, Curtis AS. Surface modified superparamagnetic nanoparticles for drug delivery: interaction studies with human fibroblasts in culture. *J Mater Sci Mater Med*. 2004;15:493–496.
25. Zhang J, Misra RD. Magnetic drug-targeting carrier encapsulated with thermosensitive smart polymer: core-shell nanoparticle carrier and drug release response. *Acta Biomater*. 2007;3:838–850.

26. Zhang JL, Srivastava RS, Misra RD. Core-shell magnetite nanoparticles surface encapsulated with smart stimuli-responsive polymer: synthesis, characterization, and lower critical solution temperature (LCST) of viable drug-targeting delivery system. *Langmuir*. 2007;23:6342–6351.
27. Zintchenko A, Ogris M, Wagner E. Temperature dependent geneexpression induced by PNIPAM-based copolymers: potential of hyperthermia in gene transfer. *Bioconjug Chem.* 2006;17:766–772.
28. Chilkoti A, Dreher MR, Meyer DE, Raucher D. Targeted drug delivery by thermally responsive polymers. *Adv Drug Deliv Rev*. 2002;54:613–630.
29. Meyer DE, Shin BC, Kong GA, Dewhirst MW, Chilkoti A. Drug targeting using thermally responsive polymers and local hyperthermia. *J Control Release.* 2001;74:213–224.
30. Hu Z, Huang G. A new route to crystalline hydrogels, guided by a phase diagram. *Angew Chem Int Ed Engl*. 2003;42:4799–4802.
31. Rahimi M, Kilaru S, Hajj S, et al. Synthesis and characterization of thermo-sensitive nanoparticles for drug delivery applications. *J Biomed Nanotechnol*. 2008;4:1–9.
32. Peppas LB, Blanchette JO. Nanoparticle and targeted systems for cancer therapy. *Adv Drug Deliv Rev.* 2004;56:1649–1659.
33. Ren J, Jia MH, Ren TB, Yuan WZ, Tan QG. Preparation and characterization of PNIPAAm-b-PLA/ Fe_3O_4 thermo-responsive and magnetic composite micelles. *Mater Lett*. 2008;62:4425–4427.
34. Yang Yong, Yongxiao Bai, Yanfeng Li, Lei Lin , Yanjun Cui, Chungu Xia. Preparation and application of polymer-grafted magnetic nanoparticles for lipase immobilization. *J Magn Magn Mater*. 2008;320:2350– 2355.
35. Rahimi M, Wadajkar A, Subramanian K, et al. In vitro evaluation of novel polymer-coated magnetic nanoparticles for controlled drug delivery. *Nanomedicine*. 2010;6:672–680.
36. Wu CL, He H, Gao HJ, et al. Synthesis of Fe_3O_4@SiO_2@polymer nanoparticles for controlled drug release. *Science China Chemistry*. 2010;53:514–518.
37. Nattama S, Rahimi M, Wadajkar AS, et al. Characterization of polymer coated magnetic nanoparticles for targeted treatment of cancer. Engineering in Medicine and Biology Workshop. Dallas, TX: IEEE; 2007. 35–38. doi:10.1109/EMBSW.2007.4454167.
38. Butoescu N, Jordan O, Burdet P, et al. Dexamethasone-containing biodegradable superparamagnetic microparticles for intra-articular administration: physicochemical and magnetic properties, in vitro and in vivo drug release. *Eur J Pharm Biopharm*. 2009;72:529–538.
39. Butoescu N, Seemayer CA, Foti M, Jordan O, Doelker E. Dexamethasone-containing PLGA superparamagnetic microparticles as carriers for the local treatment of arthritis. *Biomaterials*. 2009;30:1772–1780.
40. Perez JM, O'Loughin T, Simeone FJ, Weissleder R, Josephson L. DNA-based magnetic nanoparticle assembly acts as a magnetic relaxation nanoswitch allowing screening of DNA-cleaving agents. *J Am Chem Soc*. 2002;124:2856–2857.
41. Kinsella JM, Jimenez RJ, Ellington AD. Calorimetric detection of duplex DNA functionalized gold nanoparticles. *J Am Chem Soc*. 2005;127:3276–3277.
42. Xu CJ, Xu KM, Gu HW, et al. Dopamine as a robust anchor to immobilize functional molecules on the iron oxide shell of magnetic nanoparticles. *J Am Chem Soc*. 2004;126:9938–9939.
43. Kim J, Lee JE, Lee J, et al. Magnetic fluorescent delivery vehicle using uniform mesoporous silica spheres embedded with monodispersed magnetic and semiconductor nanocrystals. *J Am Chem Soc*. 2006;128:688–689.
44. Lu AH, Salabas EL, Schüth F. Magnetic nanoparticles: synthesis, protection, functionalization, and application. *Angew Chem Int Ed Engl*. 2007;46:1222–1244.
45. Yang XQ, Chen YH, Yuan RX, et al. Folate-encoded and Fe_3O_4-loaded polymeric micelles for dual targeting of cancer cells. *Polymer*. 2008;48:3477–3485.
46. Chang Y, Bai YP, Teng B, Li ZL. A new drug carrier: magnetite nanoparticles coated with amphiphilic block copolymer. *Chin Sci Bull*. 2009;54:1190–1196.
47. Hu FX, Neoh KG, Kang ET. Synthesis of folic acid functionalized PLLA-b-PPEGMA nanoparticles for cancer cell targeting. *Macromol Rapid Commun*. 2009;30:609–614.
48. Guo M, Yan Y, Zhang HK, et al. Magnetic and pH-responsive nanocarriers with multilayer core-shell architecture for anticancer drug delivery. *J Mater Chem*. 2008;18:5104–5112.
49. Lu J, Ma S, Sun JY, et al. Manganese ferrite nanoparticle micellar nanocomposites as MRI contrast agent for liver imaging. *Biomaterials*. 2009;30:2919–2928.
50. Thünemann AF, Schütt D, Kaufner L, Pison U, Möhwald H. Maghemite nanoparticles protectively coated with poly (ethyleneimine) and poly(ethylene oxide)-block-poly(glutamic acid). *Langmuir*. 2006;22:2351–2357.
51. Zintchenko A, Ogris M, Wagner E. Temperature dependent gene expression induced by PNIPAM-based copolymers: potential of hyperthermia in gene transfer. *Bioconjug Chem*. 2006;17:766–772.
52. Meyer DE, Shin BC, Kong GA, Dewhirst MW, Chilkoti A. Drug targeting using thermally responsive polymers and local hyperthermia. *J Control Release*. 2001;74:213–224.
53. Chen FH, Gao Q, Ni JZ. Polymer grafting and release behavior of doxorubicin from Fe_3O_4@SiO_2 core-shell structure nanoparticles via an acid cleaving amide bond: the potential for magnetic targeting drug delivery. *Nanotechnology*. 2008;19:335103
54. Santra S, Tapec R, Theodoropoulou N, Dobson J, Hebard A, Tan WH. Synthesis and characterization of silica-coated iron oxide nanoparticles in microemulsion: the effect of nonionic surfactants. *Langmuir*. 2001;17:2900–2906.
55. Kaushik A, Khan R, Solanki PR, et al. Iron oxide nanoparticles–chitosan composite based glucose biosensor. *Biosens Bioelectron*. 2008;24:676–683.
56. Reynolds AR, Laghi IJ, Baghimi SM, Hodivala-Dilk K. Nanoparticle-mediated gene delivery to tumor vasculature. *Trends Mol Med*. 2003;9:2–4.
57. WU CaiLin, HE Huan, GAO HongJun, et al. Synthesis of Fe_3O_4@SiO_2@polymer nanoparticles for controlled drug release. 2010;53:514–518.
58. Yang J, Lee CH, Ko HJ, et al. Multifunctional magneto-polymeric nanohybrids for targeted detection and synergistic therapeutic effects on breast cancer. *Angew Chem Int Ed Engl*. 2007;46:8836–8839.
59. Yu MK, Jeong YY, Park J, et al. Drug-loaded superparamagnetic iron oxide nanoparticles for combined cancer imaging and therapy in vivo. *Angew Chem Int Ed Engl*. 2008;47:5362–5365.
60. Carmichael J, DeGraff WG, Gazdar AF, Minna JD, Mitchell JB. Evaluation of a tetrazolium-based semiautomated colorimetric assay: assessment of chemosensitivity testing. Cancer Res. 47:936-942.
61. Mohammad P, Nosratollah Z, Mohammad R, Abbas A, Javad R. The inhibitory effect of Curcuma longa extract on telomerase activity in A549 lung cancer cell line. *African Journal of Biotechnology*. 2010;9:912–919.
62. Savva M, Duda E, Huang L. A genetically modified recombinant tumor necrosis factor-alpha conjugated to the distal terminals of liposomal surface grafted poly-ethyleneglycol chains. *Int J Pharm*. 1999; 184:45–51.
63. Arbab AS, Bashaw LA, Miller BR, et al. Characterization of biophysical and metabolic properties of cells labeled with superparamagnetic iron oxide nanoparticles and transfection agent for cellular MR imaging. *Radiology*. 2003;229:838–846.
64. Mahmoudi M, Sant S, Wang B, Laurent S, Sen T. Superparamagnetic iron oxide nanoparticles (SPIONs): development, surface modification and applications in chemotherapy. *Adv Drug Deliv Rev*. 2011;63:24–46.
65. Davaran S, Entezami AA. A review on application of polymers in new drug delivery systems. *Iranian Polymer Journal*. 1994;6(4): 273–289.
66. Davaran S, Entezami AA. Synthesis and hydrolysis of modified poly vinyl alcohols containing ibuprofen pendent groups. *Iranian Polymer Journal.* 1996;5(3):188–191.